

# **Converter end-point prediction model using spectrum image analysis and improved neural network algorithm**

HONG-YUAN WEN\*, QI ZHAO, YAN-RU CHEN, MU-CHUN ZHOU, MENG ZHANG, LING-FEI XU

School of Electronic Engineering and Optoelectronic Technology,  
Nanjing University of Science & Technology, Nanjing 210094, China

\*Corresponding author: wenhongyuan@yahoo.com.cn

Aiming at the present situation of the steelmaking end-point control at home and abroad, a neural network model was established to judge the end-point. Based on the colour space conversion and the fiber spectrum division multiplexing technology, a converter radiation multi-frequency information acquisition system was designed to analyze the spectrum light and image characteristic information, and the results indicate that they are similar at early-middle stage but dissimilar when approach the steelmaking blowing end. The model was trained and forecasted by using an improved neural network correction coefficient algorithm and some appropriate variables as the model parameters. The experimental results show the proposed algorithm improves the prediction accuracy by 15.4% over the conventional algorithm in 5 s errors and the respond time is about 1.688 s, which meets the requirements of end-point judgment online.

Keywords: spectrum, image, neural network, converter, end-point.

## **1. Introduction**

The end-point control is a key operation on steelmaking blowing, and the control accuracy directly affects the final quality of the steel. At present, the middle and small converter output accounts for 70% of the total output in China [1], and the experience steelmaking method is commonly adopted on these plants [2]. The problem of this method is that the control accuracy is low and the re-blowing operation is often carried out.

Many new end-point control methods are proposed in recent years. A photoelectric detector is used to judge the end-point by the change of infrared laser beam when it passes through the furnace gas [3]. However the method is only suitable for the low carbon and short distance situation, which reduces the equipment life and limits the application. Bethlehem Steel Corporation develops one optical probe to estimate the end-point carbon by detecting the light of the furnace gas [4–5]. The method is only applicable to the low carbon and large converter; moreover, the system has the tedious

cooling equipment. The sub-lance and the furnace gas analysis device [6], which is used on some large conditional converter plants, increase target hit rate, but the cost is high. These methods cannot be used in a middle and small converter widely. Some neural network models [7–10] are founded based on the steelmaking process statistical data, and they have certain accuracy. They all take the raw material, blowing oxygen quantity and some data collected from the sub-lance as the input data. However, it is difficult to gain these data directly online and the use of sub-lance increases the cost.

Aiming at the above problems, a converter radiation multi-frequency information acquisition system was designed and it could work in the steelmaking adverse environment. The spectrum and image information were analyzed and a latent law was found. Based on the law and an improved algorithm, a BP neural network model of end-point prediction was established.

## 2. Design of the radiation multi-frequency information acquisition system

### 2.1. System principle

According to the Planck radiation law, with a certain temperature  $T$  and wavelength  $\lambda$ , the radiant emittance is

$$M_{b\lambda}(T) = 2\pi hc^2 \lambda^{-5} / (e^{hc/k\lambda T} - 1) \quad (1)$$

where  $h$  represents the Planck constant, and  $k$  and  $c$  represent the Boltzmann constant and the light velocity, respectively. Based on the formula and radiation theories, the radiation multi-frequency information acquisition system was designed. The system mainly included two parts: the optical fiber system and the image capturing system. Figure 1 illustrates the system principle diagram.

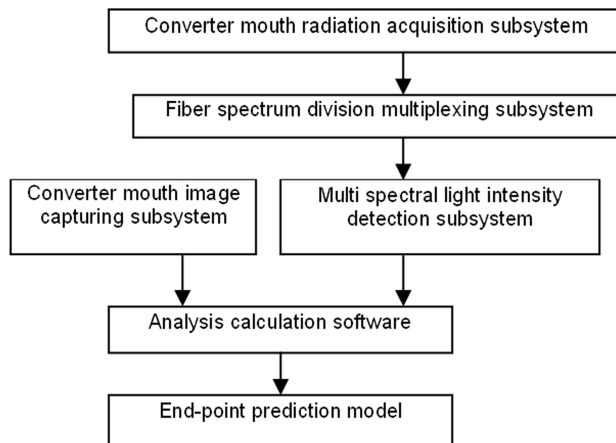


Fig. 1. System principle diagram.

Considering the converter steelmaking adverse environment, in order to acquire the converter mouth radiation information at a long distance, the method of combining the optical fiber bundle with the telescope lens was proposed. It had a good visual monitoring effect and reduced the high temperature and pollution damage to acquisition system. In view of the separated doublet, we have the following characteristics: large caliber, error correction by air-deck, adjustable relative aperture and so on. The parameters could be calculated, and Table 1 shows the results.

Table 1. Separated doublet parameters (mm).

Optical Properties	Structural Parameters		
	$r$	$d$	$n$
$f' = 1499.0$	968.3	...	1.5638
$D/f' = 1:10$	-508.2	15	Bak6
$2w = 1.2$	-508.2	0.2	1.6128
$L' = 1481.9$	-3404	19	F2

The fiber spectrum division multiplexing technology was realized based on the wavelength multiplexing theory and the optical fiber with step refractive index. Following image transmission bundle requirement, some optical fibers were combined into a thick one at one end randomly, whose cross section was matched with the exit pupil of the radiation acquisition system, and at another end they were divided into some thin fiber bundle, whose cross sections were clung to different interference filters. The filters were a part of the light intensity detection subsystem, and they could divide the whole light radiation into different wave bands. The technology could eliminate the subjective factors in the judgment and gather more comprehensive radiation information. The measurement accuracy and reliability would be increased. Ten detection points were designed based on many experiments and mathematic methods. The diameter of the filter was 10 mm and the main performance parameters were given in Table 2.

Table 2. Filter main performance parameters.

Filter number	Center Wavelength (nm)	Band Width (nm)	Peak Transmittance (%)
1	405	10	35
2	450	10	50
3	492	10	50
4	535	10	50
5	546	10	50
6	600	10	50
7	670	11	50
8	700	11	50
9	750	11	45
10	850	12	45

In order to acquire the radiation information more comprehensive and simulate the flame change rule in experience steelmaking, the converter mouth image capturing subsystem was designed to extract the flame image characteristic information by colour space conversion and DirectShow. Then the spectrum light and image characteristic information were analyzed.

## 2.2. DirectShow architecture

DirectShow is a standard media-streaming architecture on Windows platform. Figure 2 shows the relationship between an application, the DirectShow components and some of the software and hardware components that DirectShow supports.

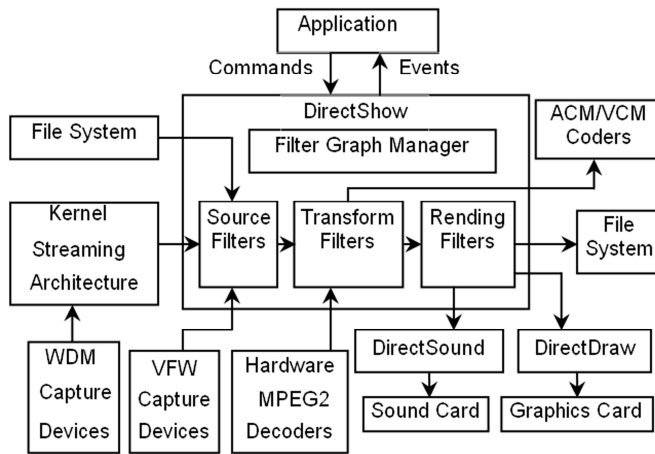


Fig. 2. DirectShow architecture.

A filter is the basic module of DirectShow, which could deal with one or more stages of processing alone. According to functions, filters can be classified into three categories: source filters, transform filters and rendering filters. A set of filters is called a filter graph, which is the most important part in DirectShow. The filter graph manager controls the filters in a filter graph.

In the research, the main steps of building filter graph are as follows: creating the filter graph, creating the capture graph builder, attaching the filter graph to the capture graph, adding capture filter to my graph, setting video window style, previewing and storing.

## 2.3. Comprehensive analysis of spectrum light and image characteristic information

The system converted the RGB data into HSV (hue, saturation, and value) colour model by the colour space conversion algorithm, which was first introduced by SMITH [11]. Considering the flame is yellow in the blowing end and the HSV colour model is a better approach to the eye perception [12], the processing method was proposed. In

HSV colour model, hue is represented by angle, and it reflects the colour information of image data directly.

The resolution of the image on the capture system is  $640 \times 480$  and the blowing is about 13 minutes. Considering the real time requirements, the system needs an efficient algorithm to process the captured data simultaneously. The colour model conversion corresponding table is proposed in this paper, which establishes the unique quantitative relation table from the RGB model to the HSV model. When one frame image is captured and each pixel is calculated by the colour space conversion algorithm, the programs will look up its correspondence position in the table and then record it automatically and quickly. The method could meet real-time requirements of the data processing.

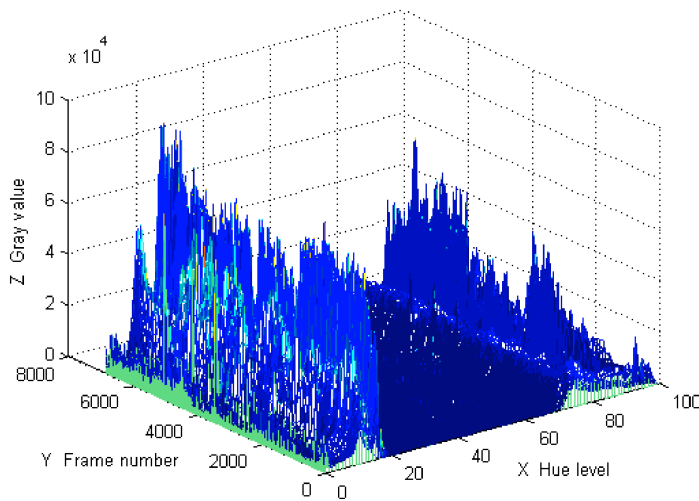


Fig. 3. Hue stereogram.

Available information should be selected from the HSV model to be used in the subsequent processing. Single frame image histogram could not reflect the whole blowing rules, therefore 3-D graph which consisted of the full frame image histogram was considered. Figure 3 shows the hue stereogram of the whole blowing process.  $X$  axis is the hue level,  $Y$  axis is the frame number, and  $Z$  axis is the gray value. 3-D graph made the mark with the colour: the more approached red, the bigger gray value was. In order to judge the end-point, the selected curve should have obvious changes when it approached the end-point. That is, we should find one or more appropriate curve on the  $XOY$  plane, which represents the hue of each frame.

When hue value was about 0.17, the colour of hue curve changed obviously with the blowing process, and red increased obviously when it approached the end-point (see Fig. 4). It indicated the curve had much potential information, especially on the end-point. The curve was selected.

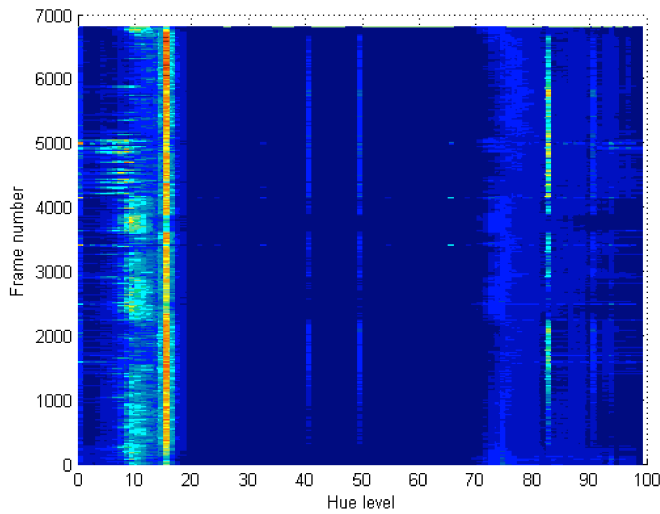


Fig. 4. Hue ichnography.

The system mainly analyzed the spectrum light at the 492 nm–535 nm wavelength spectrum section. The end-point was marked on the image curve as *E* point. The image value was much bigger than the light value, and the curves by datum adjustment and de-noise processing were shown in Fig. 5.

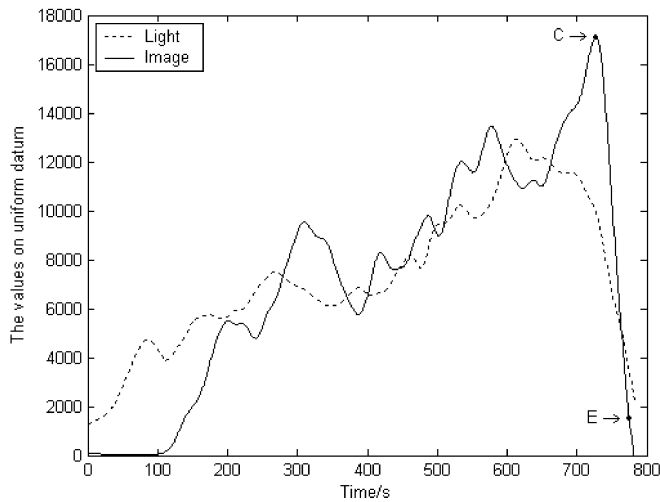


Fig. 5. The change laws of the image and light information.

The steelmaking process is a high temperature physical and chemical reaction. The light intensity value increased gradually at the beginning, fluctuated at the middle stage, and decreased slowly before the end-point. At the first two stages, the image characteristic value was similar to the light, but there was a maximum value when it

approached the end-point, which was called  $C$  point. The end-point time was affected by the raw materials and the blowing conditions, *etc.* The difference of these factors made that the different furnace end-point time was also different. The experiment found the time difference within 100 s. In order to judge the end-point, based on the above laws, an end-point mathematical model was established by using an improved neural network algorithm.

### 3. The end-point neural network prediction model

#### 3.1. BP neural network theory

BP neural network is one kind of multilayer feed forward neural networks, and consists of three layers: input layer, hidden layer, and output layer. Figure 6 shows a neural network with single hidden layer. Input nodes  $w_{ij}$  and  $w_{jl}$  respectively denote input hidden layer connection weight and hidden output layer connection weight. Back propagation (BP) learning algorithm adjusts the network weight with the signal, which is divided into working signal forward propagation and error signal back propagation. When learning sample is provided to network, the neuron response values propagate from the hidden layer to the output layer. If the output layer cannot get the desired output, the error signal will be produced. Along the negative gradient direction of the performance function, the error signal forward propagates layer by layer. The network weight and threshold are adjusted by the error feedback, and thus the target output is approximate to the expected output.

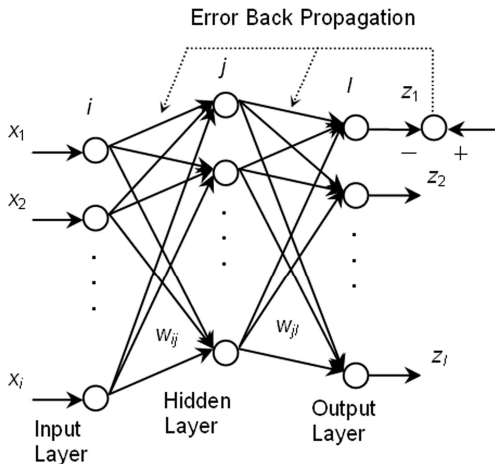


Fig. 6. The BP network structure.

#### 3.2. Algorithm deficiency and improvement

The standard BP neural network has its own deficiencies and shortcomings, which mainly include falling into the local minimum point easily, large network redundancy, fixed learning step and long training time. Adding momentum term is a conventional method to

improve BP algorithm. To get ideal training precision and short training time, the conjugate gradient method [13] is adopted in the system, whose preconstruction model would be a large complex network. To quicken the training speed, new search direction is the conjugate direction of negative gradient direction and last search direction.

If the gradient direction is  $g_0$ , the initial search direction  $p_0$  will be the negative gradient direction. One-dimensional search direction is

$$x_{k+1} = x_k + \alpha_k p_k \quad (2)$$

The conjugate direction is the new search direction

$$p_k = -g_k + \beta_k p_{k-1} \quad (3)$$

and the algorithm for the correction coefficient  $\beta_k$  is as follows:

1. Initialization. Let  $k$  be the simulation time,  $w_k$  be  $n$ -dimensional random vector and scale factor  $\lambda_b$  be 0. The influence parameter  $\sigma$  and the adjusting parameter  $\lambda$  are  $5.0e-5$  and  $5.0e-7$ , respectively.

2. Calculate the following parameters:

$$\sigma_k = \sigma / |p_k| \quad (4)$$

$$s_k = [G'(w_k + \sigma_k p_k) - G'(w_k)] / \sigma_k \quad (5)$$

$$\delta_k = p_k' s_k \quad (6)$$

3. Adjust the parameter

$$\delta_k = \delta_k + (\lambda_k - \lambda_b) \cdot |p_k|^2 \quad (7)$$

If the parameter is not more than 0, then

$$\lambda_k = 2(\lambda - 2\delta_k / |p_k|^2) p_k \quad (8)$$

$$\delta_k = -\delta_k + \lambda_k |p_k|^2 \quad (9)$$

and  $\lambda_k = \lambda_b$ .

4. Calculate the comparison parameter

$$D_k = 2\delta_k [G(w_k) - G(w_k + \alpha_k p_k)] / \mu_k^2 \quad (10)$$

where  $\mu_k = p_k' g_k$  is the step, and  $\alpha_k = \mu_k / \delta_k$ . If  $D_k$  is not more than 0, let  $w_{k+1} = w_k + \alpha_k p_k$ . If  $\text{mod}(k, n) = 0$ , restart the algorithm, or

$$\beta_{k+1} = (|g_{k+1}|^2 - g_{k+1}' g_k) / \mu_k \quad (11)$$

If  $D_k$  is more than the threshold  $\theta_1$ , then reduce the scale parameter  $\lambda_k$ . If  $D_k$  is less than the threshold  $\theta_2$ , then increase the scale parameter correspondingly. The threshold is pre-set. Recalculate and get the correction coefficient  $\beta_k$  value.

### 3.3. Network model design

The law of blowing, as written above, has been extracted and described. Because the research purpose is to judge the end-point accurately, where the carbon content and the temperature are both in requirement range, the end-point time  $T$  is selected as the single output of the network. Considering the reaction is violent at the begging and is stable from the middle stage, select the characteristic value with less interference from the latter as the example data.

At present, there is no ideal method to select the input parameters for the neural network predication model, and the general method is based on the designer's experience. In this paper, the method is as following:

If  $m$ ,  $h$  and  $z$  represent the input parameters number, the hidden layer neurons number and the network output respectively, then  $h_r$  is the output of the hidden layer on  $r$  node and  $H_r$  is that of the output layer. The influence value of the input node  $s$  to the hidden node  $r$  is performed by  $G_{rs} = Cov(h_r, x_s)w_{rs} / Var(h_r)$  and the influence value of the hidden node  $r$  to the output is given by  $g_r = Cov(H_r, z)w_r / Var(H_r)$ . Thus the influence value of the input to the output can be written as  $Q_s = \sum G_{rs}g_r$ . If the sum of  $n$  parameters' influence values is over 90% of the total, the  $n$  parameters can be selected as the input parameters of the network.

After analysis and comparison, the following seven variables are taken as the input parameters: the image characteristic mean of some time quantum  $x_1$ , the spectrum light mean  $x_2$ , the ratio  $x_3$  (between  $x_1$  and  $x_2$ ), the image value on C point  $x_4$ , the light value on C point  $x_5$ , the ratio  $x_6$  (between  $x_4$  and  $x_5$ ), and the time on C point  $x_7$ .

The dimension of every variable is different. To avoid the big eigenvalue monopolizing the learning process, the parameters were normalized with the form  $x'_i = (x_i - x_{\min}) / (x_{\max} - x_{\min})$ , where  $x_i$  is the original value,  $x'_i$  is the normalization value, and  $x_{\min}$  and  $x_{\max}$  are the minimum and maximum of the example data, respectively. Three-layer neural network with sigmoid nonlinear function can approximate rational function by arbitrary precision [14]. By continuous comparison, the result is relative ideal when the hidden layer has 8 neurons. The network model has three layers, and the node number of every layer is 7, 8, and 1, respectively. The transfer function of an output layer is Purelin function  $f_2(\text{net}_l) = \lambda' \cdot \text{net}_l$  and the transfer function of a hidden layer is Tansig function  $f_1(\text{net}_j) = 2 / [1 + \exp(-\lambda \cdot \text{net}_j)] - 1$ .

### 3.4. Experimental results

Considering the real-time requirements, the target of training precision is set at 0.001, and the batch processing, whose error convergence condition is relative simple, is selected as the training mode. 49 groups of collected data are trained according to the

above model, and one train time is marked as one Epoch. Other 26 groups of collected data are used to test model. Figure 7 shows the network training process. The training precision meets the expected requirement when the training time is 127. The training results are shown in Fig. 8.

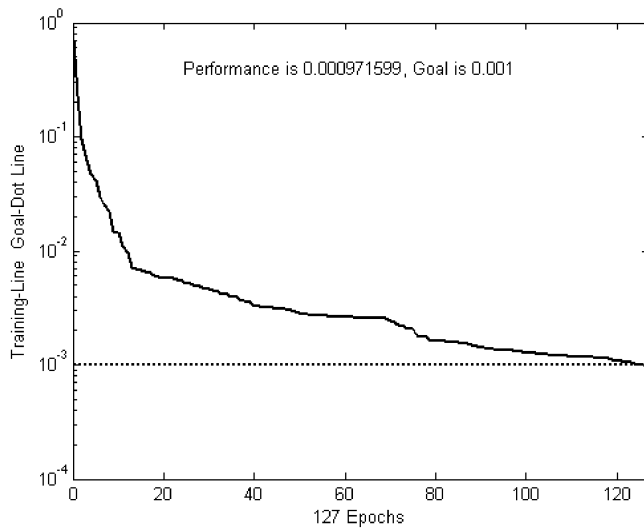


Fig. 7. Training process.

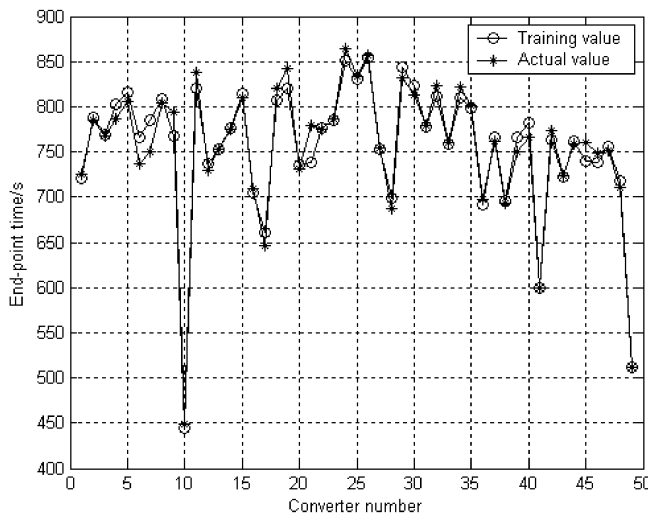


Fig. 8. The distribution graph of the training value and the actual end-point value.

Table 3 represents the comparison between the conventional algorithm with the momentum term and the proposed algorithm for the model. The proposed algorithm improves the prediction accuracy by 15.4% over the conventional algorithm when the

prediction error is lower than 5 s. The response time of the proposed algorithm is about 1.688 s and it is lower than that of the conventional algorithm and the time interval between the  $x_7$  and the end-point. The experimental results show the network model meet the time requirements of the fast end-point judgment.

Table 3. The comparison between the proposed algorithm and the conventional algorithm.

Method	Training (49groups)			Prediction Error (26 groups)	
	Training Error		Time	<5s	<10s
	<5s	<10s	(s)	<5s	<10s
Proposed algorithm	75.5%	83.7%	1.688	76.9%	84.6%
Conventional algorithm	61.2%	71.4%	3.241	61.5%	73.1%

## 4. Conclusions

In this paper, we have presented a method using the radiation multi-frequency information and improved neural network to judge the steelmaking end-point. Based on the fiber spectrum division multiplexing technology and DirectShow technology, an acquisition system was designed. The spectrum light and image characteristic information were mainly researched, and the latent law with blowing was founded. Several appropriate parameters were selected from the law curves and then the end-point neural network model was established by using an improved network algorithm.

The system was different from with the above methods; it could work in the steelmaking adverse environment without cooling equipment and collect the data quickly online without the sub-lance. The experimental results show that the proposed algorithm is superior to the conventional algorithm. The training precision and the prediction accuracy are both more than 75% in 5 s errors. The respond time is about 1.688 s, and it meets the requirements of end-point judgment online. To get better prediction accuracy, more experimental data are needed to adjust the model.

*Acknowledgments* – We thank Nanjing Iron & Steel Group Co., Ltd for assistance with the experiments. This work is supported by the National High Tech Research and Development Program of China (2007AA04Z181), the Natural Science Foundation of China (Grant No. 50176020) and the High-tech Development Project (Industry Part) of Jiangsu Province (Grant No. BG2005006).

## References

- [1] LIU L., *Technical progress in converter steelmaking in China*, Iron and Steel **40**(2), 2005, pp. 1–5.
- [2] WANG M.H., HUI Z.G., Shi X.L., *End-point Control Technology of Converter*, Angang Technology **333**(3), 2005, pp. 6–10.
- [3] MERRIMAN D., *Mass spectrometry for oxygen steel-making control*, Steel Times **225**(11), 1997, pp. 439–40.
- [4] SHARAN A., *Light sensors for BOF carbon control in low carbon heats*, [In] *Steelmaking Conference Proceedings*, Toronto, Canada: ISS, **81**, 1998, pp. 337–45.

- [5] SHARAN A., *Fiber optic sensor and method of use thereof to determine carbon content of molten steel contained in a basic oxygen furnace*, US, 6175676[P], 2001, 1–16.
- [6] WANG Y., YANG N.C., WANG C.K., *Present situation and development of converter steelmaking in China*, *Special Steel* **26**(4), 2005, pp. 1–5.
- [7] YUN S.Y., CHANG K.S., *Dynamic prediction using neural network for automation of BOF process in steel industry*, *Iron and Steelmaker* **23**(8), 1996, pp. 37–42.
- [8] DING R., LIU L., *Artificial intelligence static control model in converter steelmaking*, *Iron and Steel* **32**(1), 1997, pp. 22–6.
- [9] XIE S.M., TAO J., CHAI T.Y., *BOF steelmaking endpoint control based on network*, *Control Theory and Applications* **20**(6), 2003, pp. 903–7.
- [10] WANG Z.J., CHAI T.Y., SHAO C., *Slab minierature prediction model based on RBF neural network*, *Journal of System Simulation* **11**(3), 1999, pp. 181–4.
- [11] SMITH A.R., *Color gamut transformation pairs*, *Computer Graphics*, **12**(3), 1978, pp. 12–9.
- [12] GONZALEZ R.C., WOODS R.E., EDDINS S.L., *Digital Image Processing Using MATLAB*, Shaddle River, New Jersey, US: Prentice Hall, 2004.
- [13] CHEN K.Z., *Optimized Arithmetic*, Xi'an: Northwestern Polytechnic University Press, 2001.
- [14] HORNIK K., STINCHCOMBE M., WHITE H., *Multilayer feedforward networks are universal approximators*, *Neural Network*, **2**(5), 1989, pp. 359–66.

*Received November 27, 2007  
in revised form March 3, 2008*